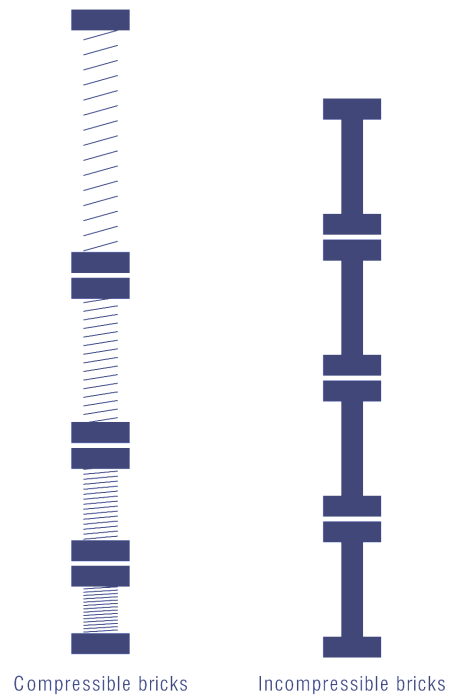


# The Atmosphere



# Atmospheric Pressure



**Figure 5-6** A wall made of compressible bricks, to demonstrate why pressure changes rapidly at the bottom of the atmosphere and slowly at the top because air in the atmosphere is compressible (*left*). For water, which is incompressible, pressure increases linearly with depth.

**Table 3.1** Composition of the Atmosphere<sup>a</sup>

Constituent	Chemical Formula	Molecular Weight ( <sup>12</sup> C=12)	Percent by Volume in Dry Air	Total Mass (g)
Total atmosphere				$5.136 \times 10^{21}$
Water vapor	H <sub>2</sub> O	18.01534	variable	$0.017 \times 10^{21}$
Dry air		28.9644	100.0	$5.119 \times 10^{21}$
Nitrogen	N <sub>2</sub>	28.0134	78.084	$3.866 \times 10^{21}$
Oxygen	O <sub>2</sub>	31.9988	20.948	$1.185 \times 10^{21}$
Argon	Ar	39.948	0.934	$6.59 \times 10^{19}$
Carbon dioxide	CO <sub>2</sub>	44.00995	0.0315	$2.45 \times 10^{18}$
Neon	Ne	20.183	$1.818 \times 10^{-3}$	$6.48 \times 10^{16}$
Helium	He	4.0026	$5.24 \times 10^{-4}$	$3.71 \times 10^{15}$
Methane	CH <sub>4</sub>	16.04303	$\sim 1.5 \times 10^{-4}$	$\sim 4.3 \times 10^{15}$
Hydrogen	H <sub>2</sub>	2.01594	$\sim 5 \times 10^{-5}$	$\sim 1.8 \times 10^{14}$
Nitrous oxide	N <sub>2</sub> O	44.0128	$\sim 3 \times 10^{-5}$	$\sim 2.3 \times 10^{15}$
Carbon monoxide	CO	28.0106	$\sim 1.2 \times 10^{-5}$	$\sim 5.9 \times 10^{14}$
Ammonia	NH <sub>3</sub>	17.0306	$\sim 1 \times 10^{-6}$	$\sim 3 \times 10^{15}$
Nitrogen dioxide	NO <sub>2</sub>	46.0055	$\sim 1 \times 10^{-7}$	$\sim 8.1 \times 10^{12}$
Sulfur dioxide	SO <sub>2</sub>	64.063	$\sim 2 \times 10^{-8}$	$\sim 2.3 \times 10^{12}$
Hydrogen sulfide	H <sub>2</sub> S	34.080	$\sim 2 \times 10^{-8}$	$\sim 1.2 \times 10^{12}$
Ozone	O <sub>3</sub>	47.9982	Variable	$\sim 3.3 \times 10^{15}$

<sup>a</sup> From Walker (1977). Schlesinger 1991

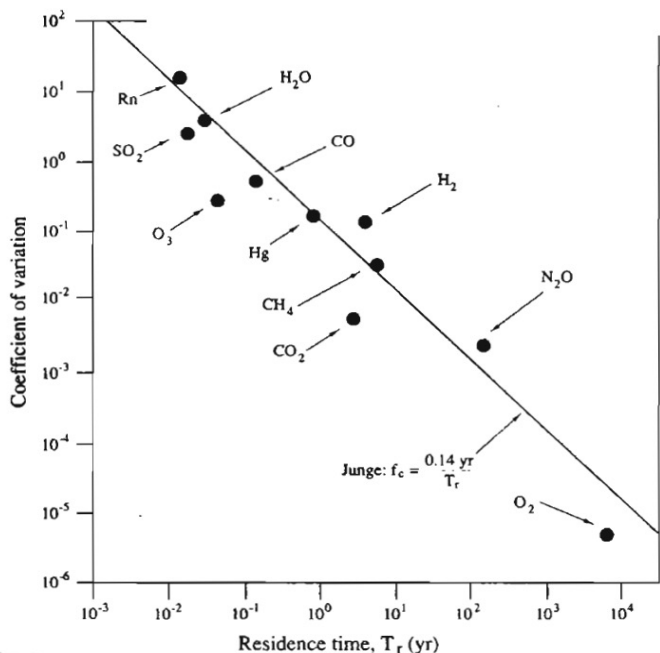


**Figure 3.4** Variability in the concentration of atmospheric gases (expressed as the coefficient of variation in measurements) as a function of their estimated mean residence times in the atmosphere. From Junge (1974), as updated by Slinn (1988). Schlesinger 1991

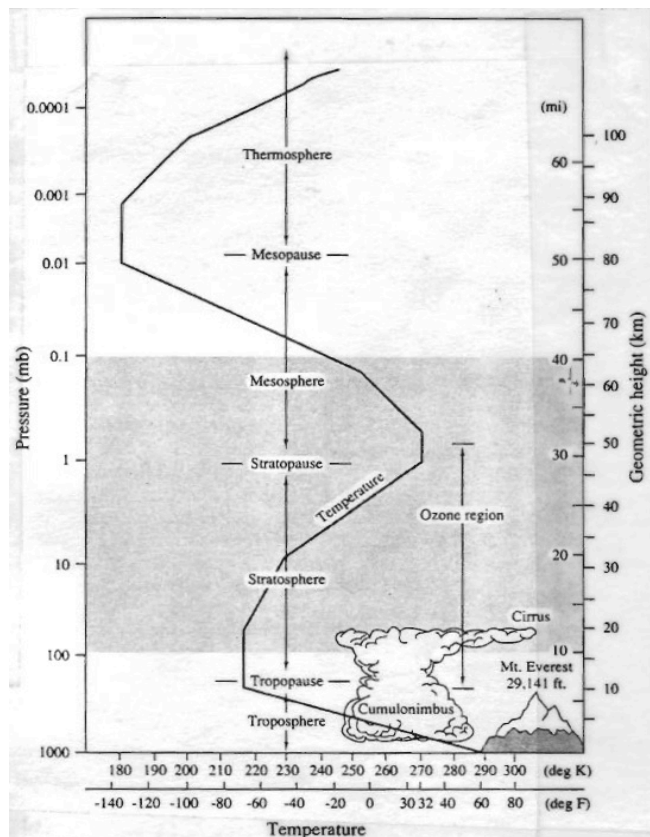


**Figure 3.2** Temperature profile of the atmosphere to 100 km.

Schlesinger 1991

TABLE 4-2 THE ATMOSPHERE PROBLEM (ASSUMES 20% OXYGEN)\*

Gas	Abundance	Expected equilibrium concentration	Discrepancy	Residence time (yrs)	Output (10 <sup>6</sup> tons/yr)
Nitrogen	0.8	10 <sup>-10</sup>	10 <sup>9</sup>	3 × 10 <sup>6</sup>	1,000
Methane	1.5 × 10 <sup>-6</sup>	<10 <sup>-35</sup>	10 <sup>29</sup>	7	2,000
Nitrous oxide	3 × 10 <sup>-7</sup>	10 <sup>-20</sup>	10 <sup>13</sup>	10	600
Ammonia	1 × 10 <sup>-8</sup>	<10 <sup>-35</sup>	10 <sup>27</sup>	.01	1,500
Methyl iodide	1 × 10 <sup>-12</sup>	<10 <sup>-35</sup>	10 <sup>23</sup>	.001	30
Hydrogen	5 × 10 <sup>-7</sup>	<10 <sup>-35</sup>	10 <sup>23</sup>	2	20

\* Calculations of J.E. Lovelock, see Lovelock 1988.

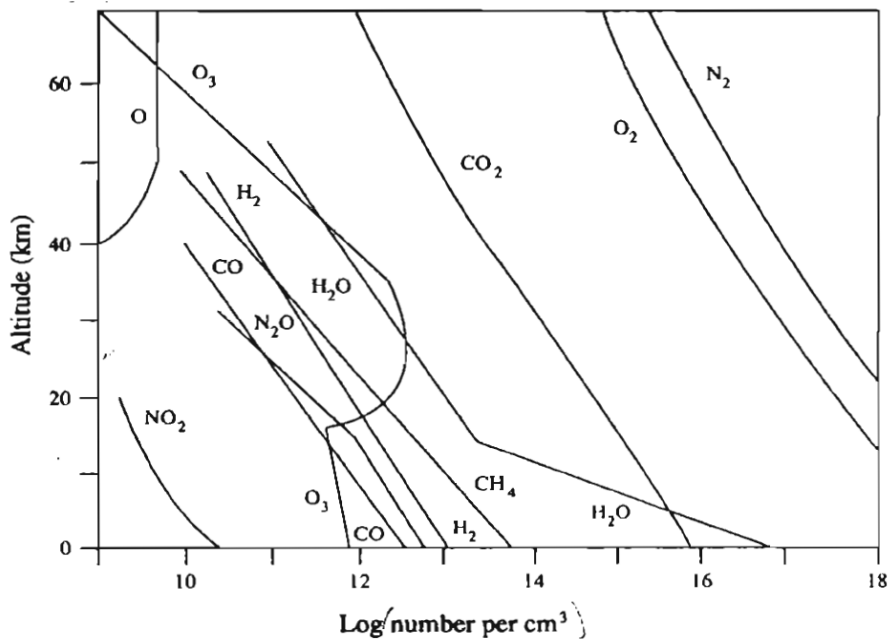


Figure 3.5 The approximate altitudinal distribution of atmospheric constituents. From Walker (1977). Schlesinger 1991

# Vertical Structure of the Heterosphere

# Sources of Atmospheric Aerosols

*(mass emissions)*

Deflation weathering → 1 - 10 um                      13 %

Sea Spray Salts → 1 – 10 um                              82 %

Sulfur Compounds → 0.1 um                              2 %

Other (soot, fire debris, organic cmpds)              3 %

~2.5 % of emissions are anthropogenic

~10 % of aerosol burden is anthropogenic

Mean Residence Time ~ 5 day.

## Effects of Aerosols

Delivers micro- & macronutrients

Examples:

Fe to the Ocean

P to the Amazon

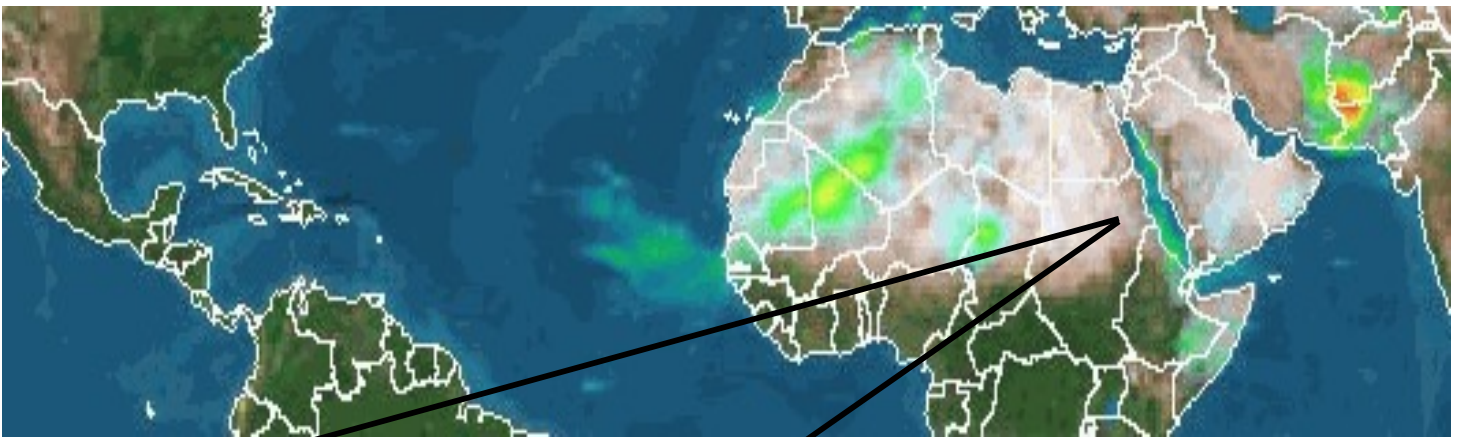
Reflects solar radiation

Serve as condensation nuclei for rain drop formation

Serve as reaction sites for some chemical reactions

# Aerosols transport materials

*From land to sea*  
*From continent to continent*  
*From the sea to land*



# High Nutrient, Low Chlorophyll (HNLC)

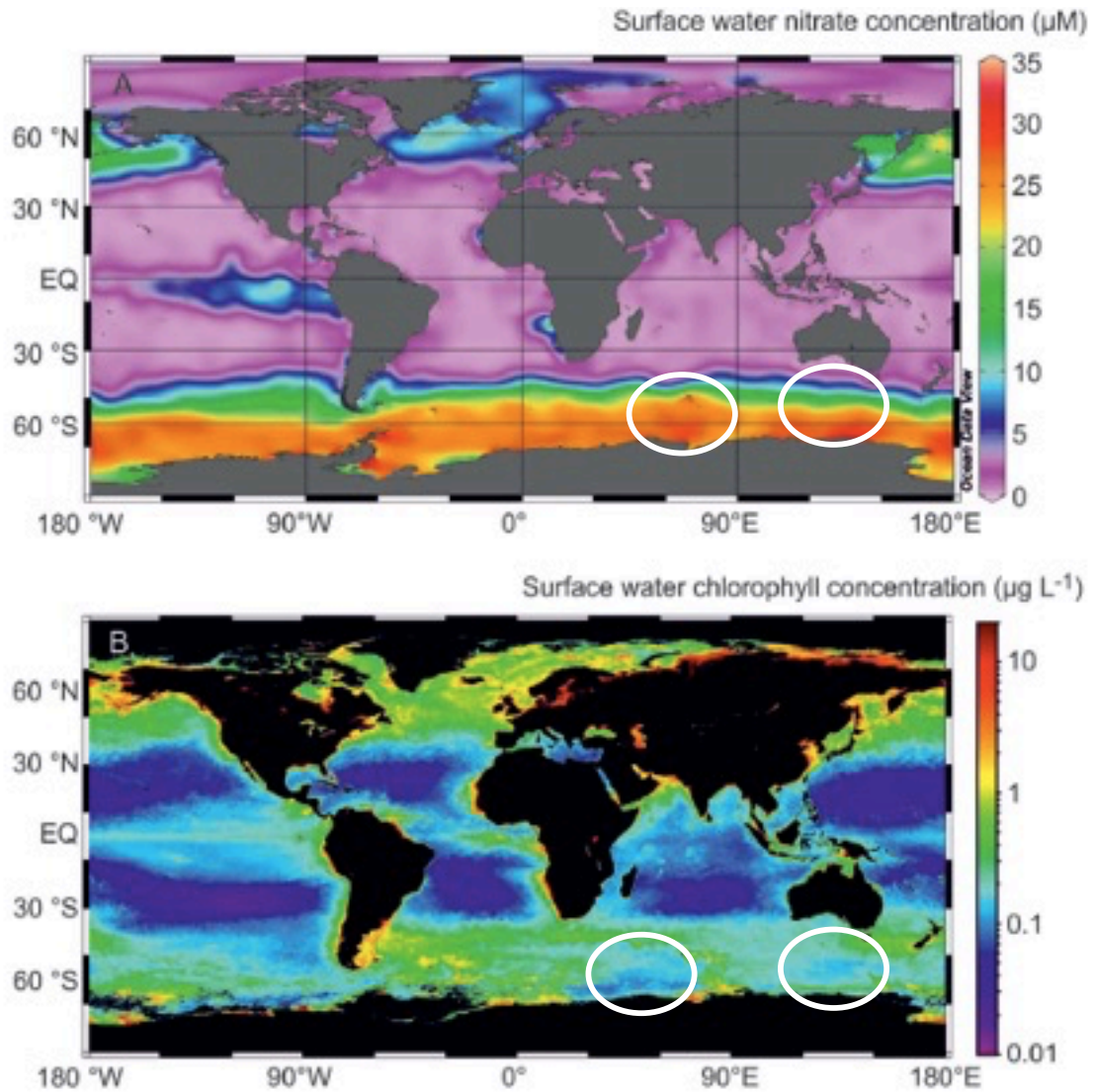


**FIGURE 1** | (A) Annualized average nitrate ( $\mu\text{M}$ ) and (B) composite chlorophyll *a* ( $\text{mg L}^{-1}$ ) distributions observed in surface waters in the global ocean. The nitrate distribution was obtained using data from the World Ocean Atlas 2009

([http://www.nodc.noaa.gov/OCS/WOA09/pr\\_woa09.html](http://www.nodc.noaa.gov/OCS/WOA09/pr_woa09.html)), while the chlorophyll *a* distribution represents the 2009 Aqua MODIS chlorophyll composite (<http://oceancolor.gsfc.nasa.gov/cgi/l3>).

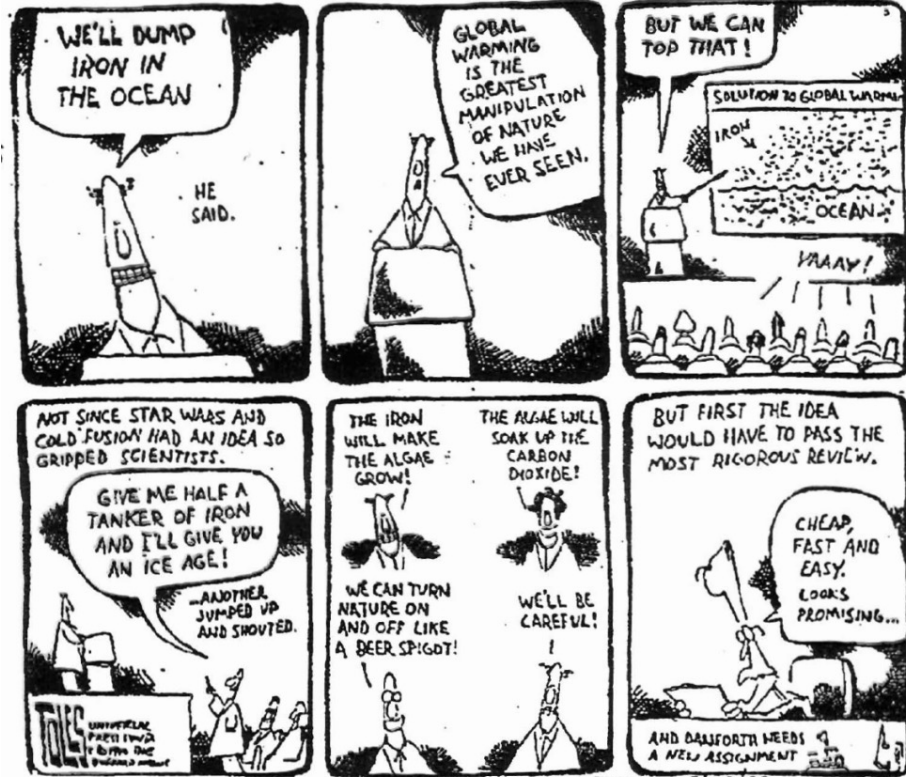


A New Iron Age, Or A Ferric Fantasy



Illustration by E. Paul Oberlander

US. JGOS Newsletter April 1990



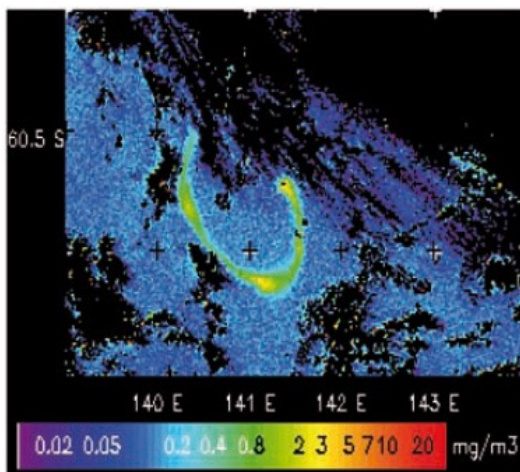
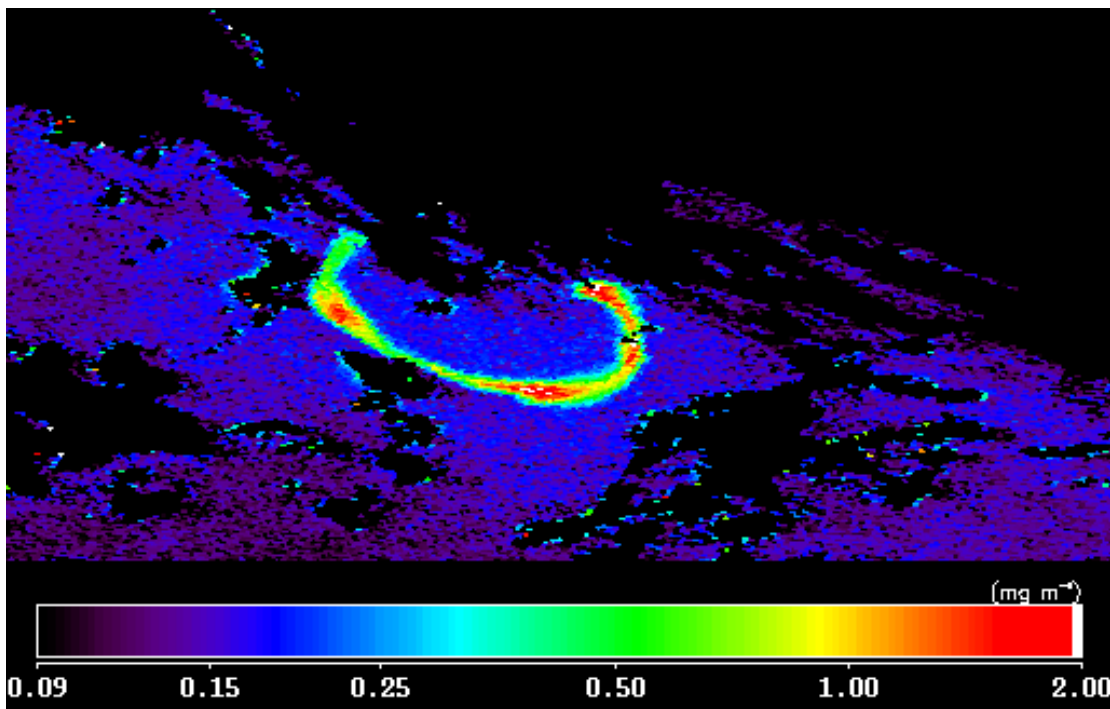


Figure 3: A NASA ocean colour image over the Southern Ocean south of Australia showing a patch of elevated chlorophyll 150km long covering  $\sim 1000\text{km}^2$  at 40 days after iron-fertilisation during the New Zealand SOIREE iron experiment in January 1999. b) A microscope image of the diatom *Fragilariopsis kerguelensis*, the diatom species that bloomed during the SOIREE iron experiment.

## OCEAN CHEMISTRY

# Iron Fertilization: A Tonic, but No Cure for the Greenhouse

## REPORTS

### The Effects of Iron Fertilization on Carbon Sequestration in the Southern Ocean

Ken O. Buesseler,\* John E. Andrews,  
Steven M. Pike, Matthew A. Charette

An unresolved issue in ocean and climate sciences is whether changes to the surface ocean input of the micronutrient iron can alter the flux of carbon to the deep ocean. During the Southern Ocean Iron Experiment, we measured an increase in the flux of particulate carbon from the surface mixed layer, as well as changes in particle cycling below the iron-fertilized patch. The flux of carbon was similar in magnitude to that of natural blooms in the Southern Ocean and thus small relative to global carbon budgets and proposed geoengineering plans to sequester atmospheric carbon dioxide in the deep sea.

As the largest high nutrient–low chlorophyll region, the Southern Ocean was chosen for a purposeful iron fertilization experiment,

SOFeX (Southern Ocean Iron Experiment). The experiment was conducted at two sites both north and south of the Antarctic Polar

Front, in low- and high-silicate waters, respectively. We focus here on the “southern patch” where the inert tracer SF<sub>6</sub> and four enrichments of iron were added to a 15 km by 15 km patch (66°S, 172°W), which was tracked and monitored by three ships in a Lagrangian fashion for 1 month in January to February 2002. As in previous experiments (1–3), the addition of the essential micronutrient iron led to measurable decreases in dissolved inorganic carbon and nutrients within the surface mixed layer (upper 40 to 50 m) associated with enhanced growth of marine phytoplankton, the details of which are described in the accompanying article by Coale *et al.* (4).

Department of Marine Chemistry and Geochemistry,  
Woods Hole Oceanographic Institution, Woods Hole,  
MA 02543, USA.

\*To whom correspondence should be addressed. E-mail: kbuesseler@whoi.edu

# Southern Ocean dust–climate coupling over the past four million years

Alfredo Martínez-García<sup>1,2,3</sup>, Antoni Rosell-Melé<sup>3,4,5</sup>, Samuel L. Jaccard<sup>1</sup>, Walter Geibert<sup>6,7</sup>, Daniel M. Sigman<sup>8</sup> & Gerald H. Haug<sup>1,2</sup>

Dust has the potential to modify global climate by influencing the radiative balance of the atmosphere and by supplying iron and other essential limiting micronutrients to the ocean<sup>1,2</sup>. Indeed, dust supply to the Southern Ocean increases during ice ages, and ‘iron fertilization’ of the subantarctic zone may have contributed up to 40 parts per million by volume (p.p.m.v.) of the decrease (80–100 p.p.m.v.) in atmospheric carbon dioxide observed during late Pleistocene glacial cycles<sup>3–7</sup>. So far, however, the magnitude of Southern Ocean dust deposition in earlier times and its role in the development and evolution of Pleistocene glacial cycles have remained unclear. Here we report a high-resolution record of dust and iron supply to the Southern Ocean over the past four million years, derived from the analysis of marine sediments from ODP Site 1090, located in the Atlantic sector of the subantarctic zone. The close correspondence of our dust and iron deposition records with Antarctic ice core reconstructions of dust flux covering the past 800,000 years (refs 8, 9) indicates that both of these archives record large-scale deposition changes that should apply to most of the Southern Ocean, validating previous interpretations of the ice core data. The extension of the record beyond the interval covered by the Antarctic ice cores reveals that, in contrast to the relatively gradual intensification of glacial cycles over the past three million years, Southern Ocean dust and iron flux rose sharply at the Mid-Pleistocene climatic transition around 1.25 million years ago. This finding complements previous observations over late Pleistocene glacial cycles<sup>8,9</sup>, providing new evidence of a tight connection between high dust input to the Southern Ocean and the emergence of the deep glaciations that characterize the past one million years of Earth history.

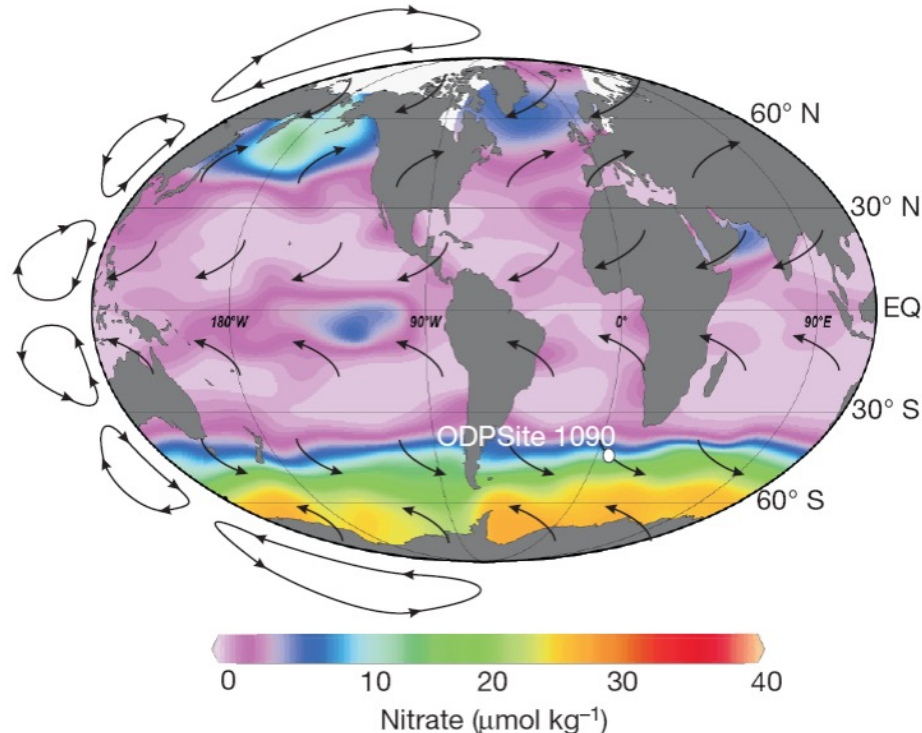


**Figure 1 | Location of ODP Site 1090, world ocean surface nitrate concentrations, and wind direction.** ODP Site 1090, the source of the sediment cores used in this study, is located at 42° 54.5' S, 8° 54.0' E, at 3,702 m depth. Nitrate concentrations are from the Electronic Atlas of the World Ocean Experiment. Black arrows are schematic representations of atmospheric convection cells and wind directions. EQ, Equator.

Table 3. Comparison of deposition fluxes ( $\text{kg ha}^{-1} \text{ yr}^{-1}$ ) of selected trace species associated with intrusions of Saharan dust and precipitation in the Amazonian wet season (December–May)

Species	Dust Intrusions <sup>a)</sup>		Precipitation <sup>b)</sup>	
	average	range	average	range <sup>c)</sup>
Na	2.1	0.80–3.4	1.7	0.73–2.9
K	0.55	0.23–0.87	1.3	0.41–2.3
NH <sub>4</sub>	0.84	0.15–1.7	0.71	0.38–1.4
Cl	3.6	2.5–4.9	2.9	1.4–5.1
NO <sub>3</sub>	3.0	0.38–4.9	1.4	0.90–3.7
SO <sub>4</sub>	4.6	0.42–7.0	1.8	1.2–3.1
PO <sub>4</sub>	0.07 <sup>d)</sup>	0.032–0.14 <sup>d)</sup>	0.04 <sup>e)</sup>	0.01–0.12 <sup>e)</sup>

<sup>a)</sup> Calculated using mass concentrations reported in Table 2.

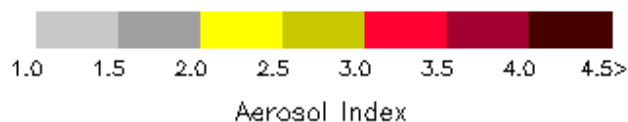
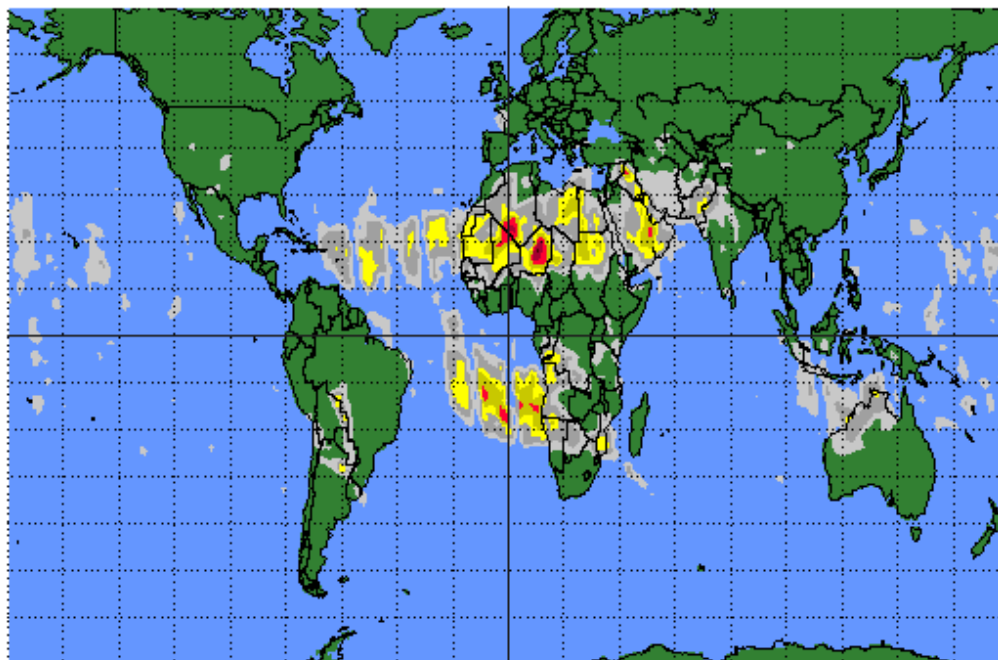
<sup>b)</sup> Based on measurements reported in Table 1 from Andreae et al. (1990).

<sup>c)</sup> Based on upper and lower quartile concentrations observed at two sites within the triangle area (Andreae et al., 1990).

<sup>d)</sup> Estimated using average mass concentration (see Table 2) reported by Talbot et al. (1986).

<sup>e)</sup> Based on unpublished data from ABLE 2b (R. Talbot and M. Andreae, personal communication, 1987). swap et al. 1992

Earth Probe TOMS Version 8 Aerosol Index on September 11, 2000

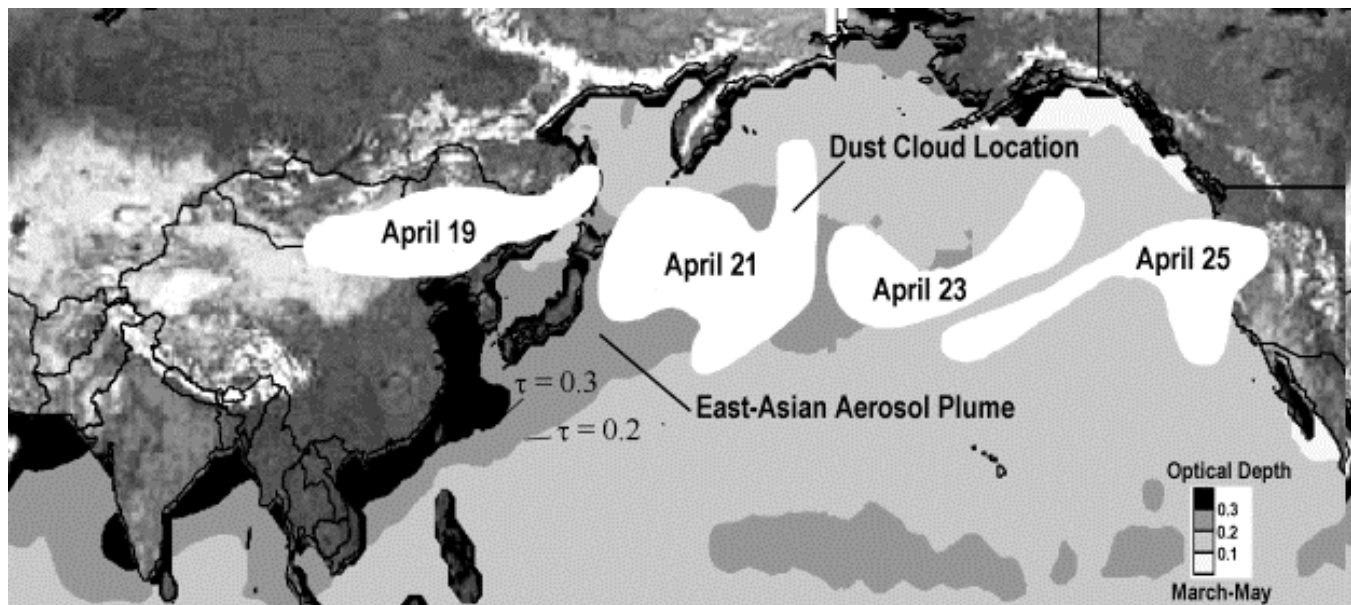


Goddard Space Flight Center

# Changing sources of nutrients during four million years of ecosystem development

O. A. Chadwick, L. A. Derry, P. M. Vitousek, B. J. Huebert & L. O. Hedin

As soils develop in humid environments, rock-derived elements are gradually lost, and under constant conditions it seems that ecosystems should reach a state of profound and irreversible nutrient depletion. We show here that inputs of elements from the atmosphere can sustain the productivity of Hawaiian rainforests on highly weathered soils. Cations are supplied in marine aerosols and phosphorus is deposited in dust from central Asia, which is over 6,000 km away.



Husar et al. 2001

# Dust from Africa can even affect air quality in Texas

## Quantifying the Contribution of Long-Range Saharan Dust Transport on Particulate Matter Concentrations in Houston, Texas, Using Detailed Elemental Analysis

Ayse Bozlaker,<sup>†</sup> Joseph M. Prospero,<sup>‡</sup> Matthew P. Fraser,<sup>§</sup> and Shankaraman Chellam<sup>\*,†,||</sup>

<sup>†</sup>Department of Civil and Environmental Engineering, University of Houston, Houston, Texas 77204, United States

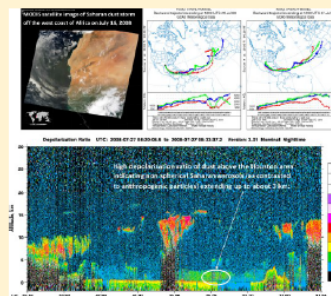
<sup>‡</sup>Rosenstiel School of Marine and Atmospheric Science, University of Miami, Miami, Florida 33149, United States

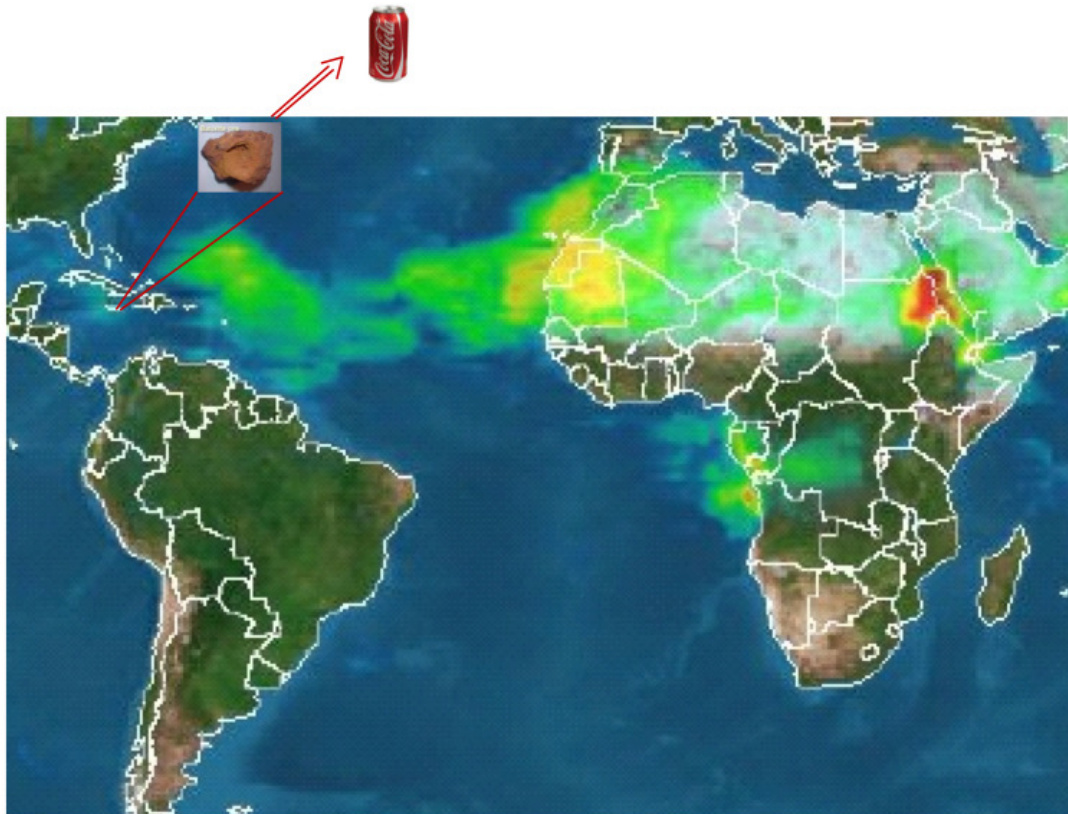
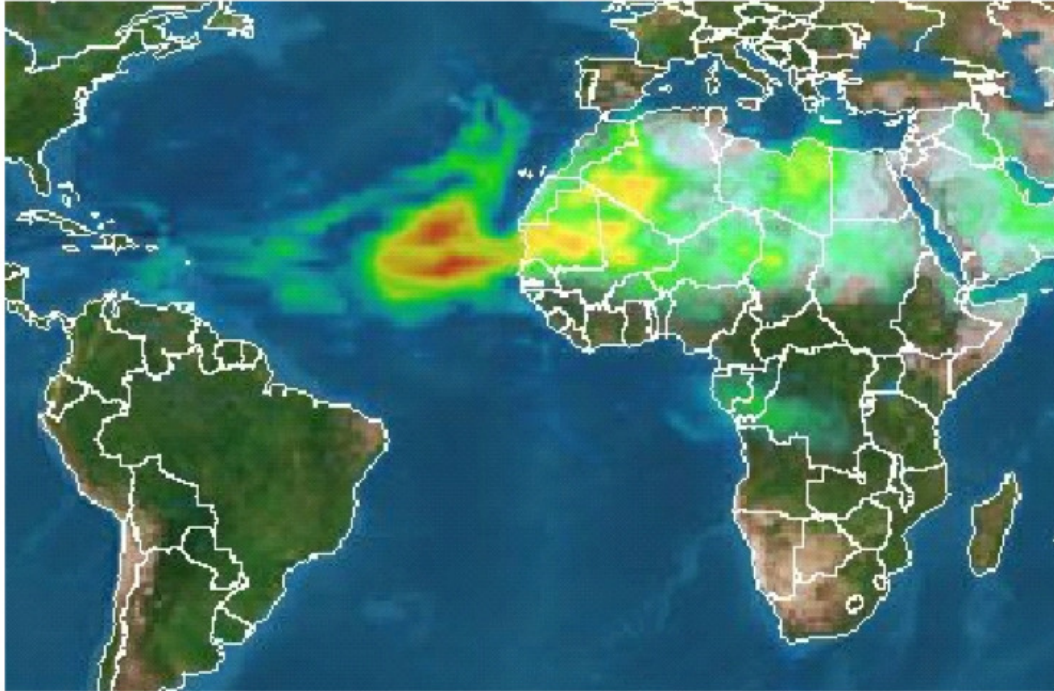
<sup>§</sup>School of Sustainable Engineering and the Built Environment, Arizona State University, Tempe, Arizona 85287, United States

<sup>||</sup>Department of Chemical and Biomolecular Engineering, University of Houston, Houston, Texas 77204, United States

**S** Supporting Information

**ABSTRACT:** The trans-Atlantic transport of North African dust by summertime trade winds occasionally increases ambient particulate matter (PM) concentrations in Texas above air quality standards. Exemptions from such exceedences can be sought for episodic events that are beyond regulatory control by providing qualitative supportive information such as satellite images and back-trajectories. Herein we demonstrate that chemical mass balancing can successfully isolate, differentiate, and quantify the relative contributions from local and global mineral dust sources through detailed measurements of a wide suite of elements in ambient PM. We identified a major dust storm originating in Northwest Africa in mid-July 2008 which eventually impacted air quality in Houston during July 25, 26, and 27, 2008. Daily PM<sub>2.5</sub> and PM<sub>10</sub> samples were collected at two sites in Houston over a 2-week period encompassing the Saharan dust episode to quantify the transported mineral dust concentrations during this peak event. Average PM concentrations more than doubled during the Saharan intrusion compared with non-Saharan. Relative concentrations of several elements often associated with anthropogenic sources were significantly diluted by crustal minerals coincident with the large-scale Saharan dust intrusion. During non-Saharan days, local mineral dust sources including cement manufacturing and soil and road dust contributed in total 26% to PM<sub>2.5</sub> mass and 50% to PM<sub>10</sub> mass; during the three-day Saharan episode the total dust contribution increased to 64% for PM<sub>2.5</sub> and 85% for PM<sub>10</sub>. Importantly, this approach was also able to determine that local emissions of crustal minerals dominated the period immediately following the Saharan dust episode: simple quantification of bulk crustal materials may have misappropriated this elevated PM to trans-Atlantic transport of Saharan dust.





[http://svs.gsfc.nasa.gov/stories/dust\\_20030715/index.html](http://svs.gsfc.nasa.gov/stories/dust_20030715/index.html)



# From the sea to land

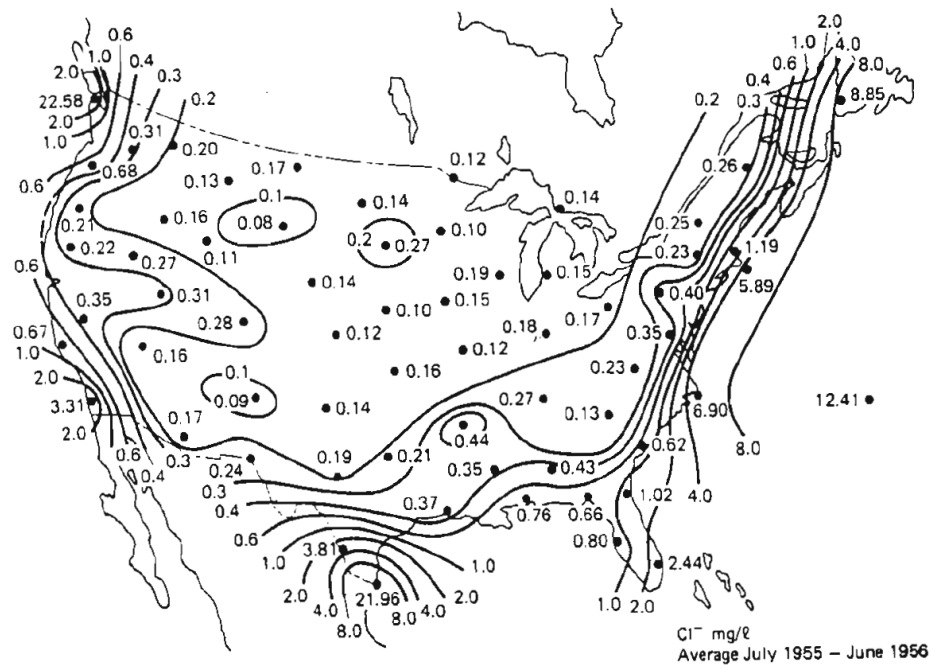
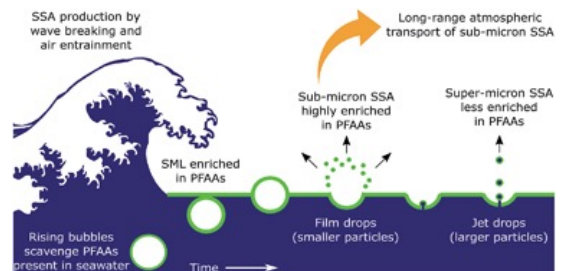
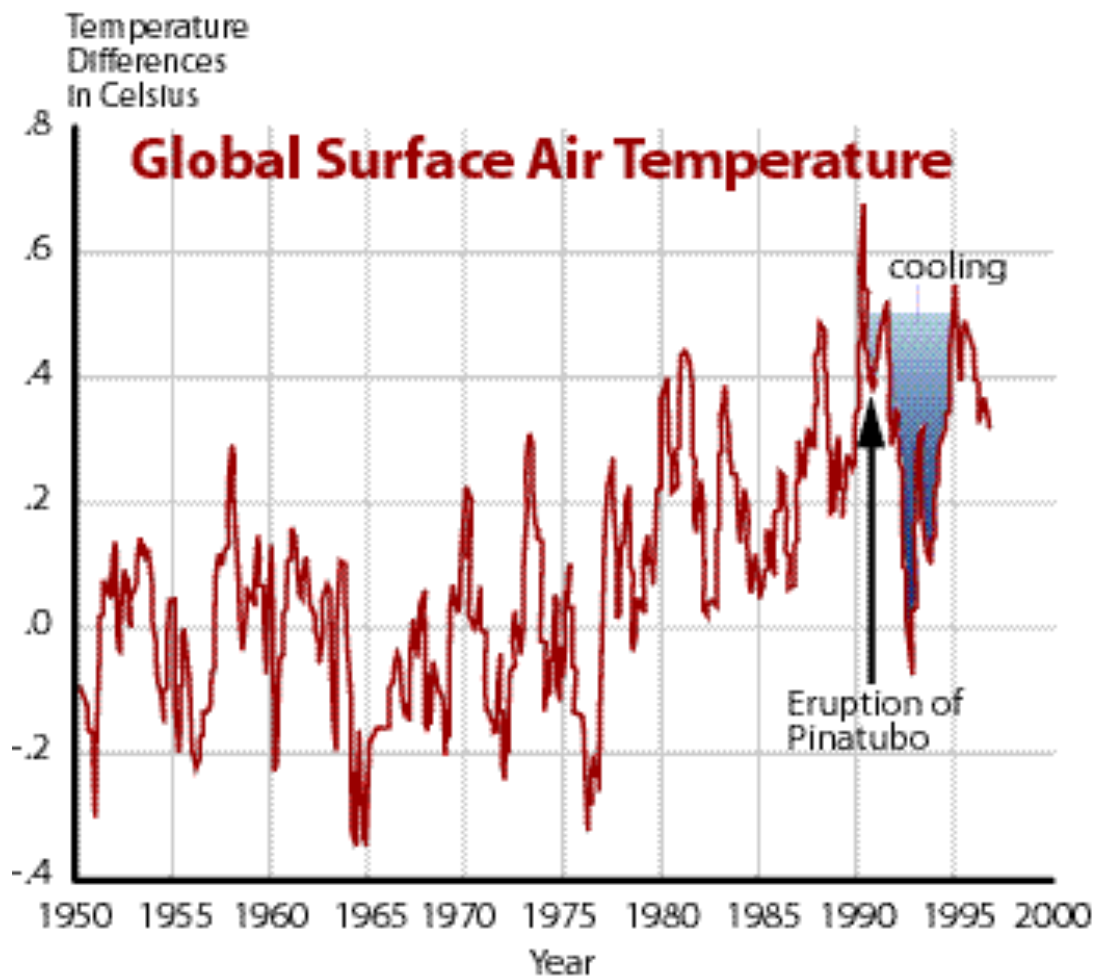
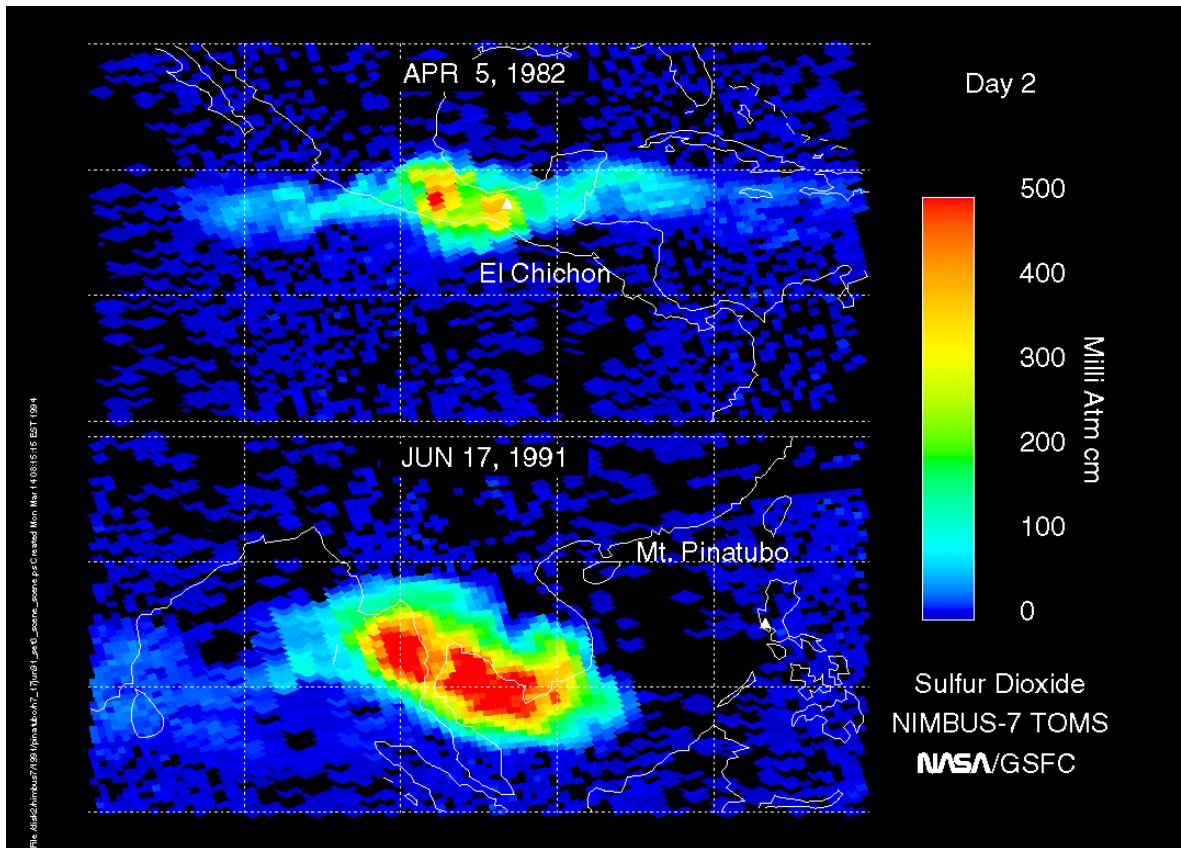


Figure 1-5 Average sodium and chloride concentrations in precipitation over the United States (Junge and Werby 1958). Dreuer 1982

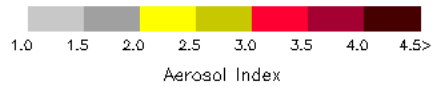
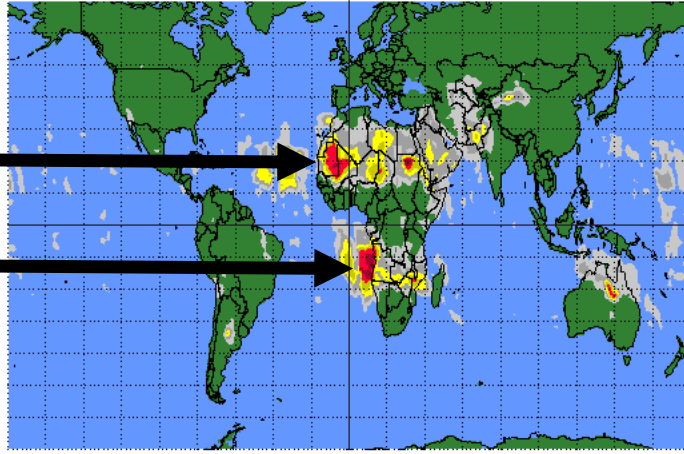


# Sulfate aerosols can reflect sunlight



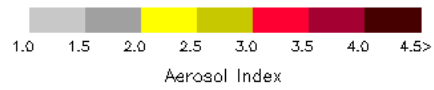
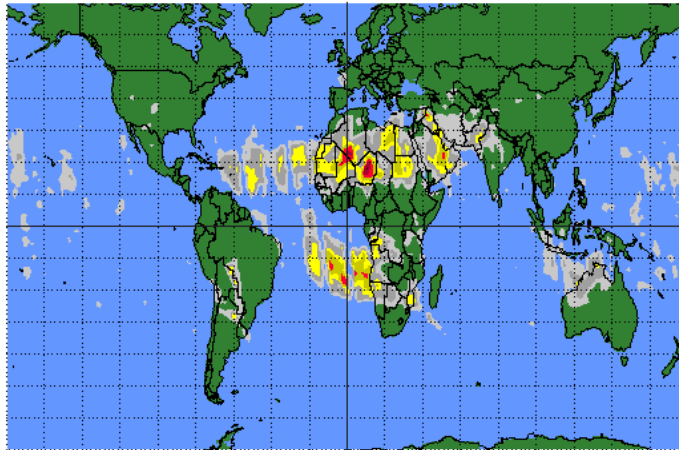
Earth Probe TOMS Version 8 Aerosol Index  
on September 08, 2000

Dust  
Smoke



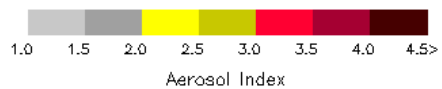
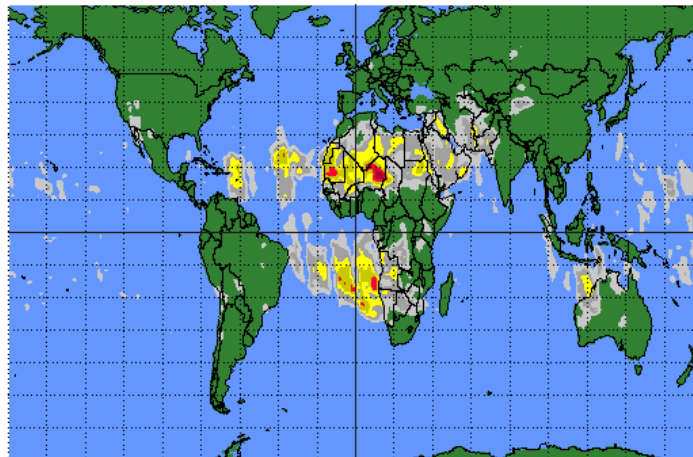
Goddard Space  
Flight Center

Earth Probe TOMS Version 8 Aerosol Index  
on September 11, 2000



Goddard Space  
Flight Center

Earth Probe TOMS Version 8 Aerosol Index  
on September 12, 2000

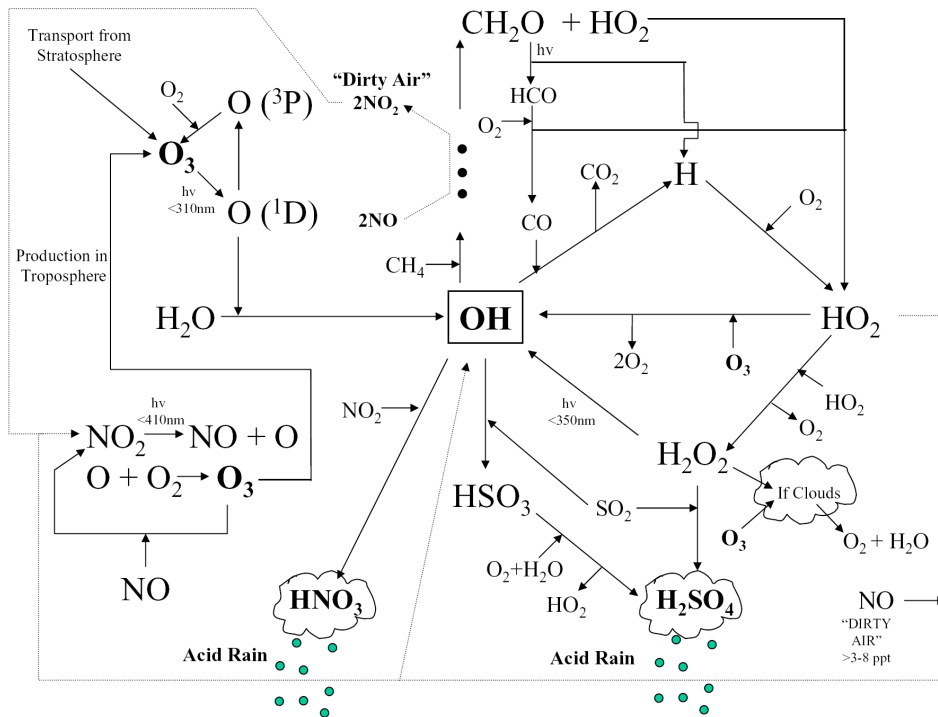


Goddard Space  
Flight Center

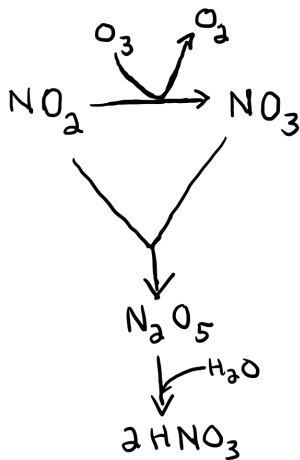
**Table 3.4** Reaction of Atmospheric Trace Gases Containing, C, N, and S with OH<sup>a</sup>

Trace gas	Mixing Ratio in the Northern Hemisphere (ppb)	Mean Tropospheric Lifetime	Contribution of OH-sink Reaction (%)
CH <sub>4</sub>	1600	10 yr	90
CO	250	60 days	100
Nonmethane hydrocarbons (NMHC), C <sub>2</sub> -C <sub>5</sub>	2-10	1-100 days	50-100
SO <sub>2</sub>	0.2	14 days	50
COS	0.5	5 yr	30
H <sub>2</sub> S		4 days	100
(CH <sub>3</sub> ) <sub>2</sub> S		1 day	50
NO, NO <sub>2</sub>	0.1	1 day	100
NH <sub>3</sub>	~1	14 days	10
N <sub>2</sub> O	310	150 yr	0

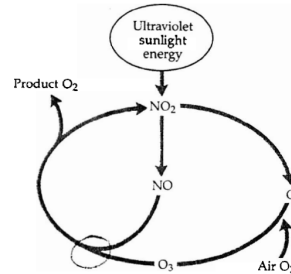
<sup>a</sup> Modified from Ehhalt (1981).



## At Night



### PHOTOLYTIC NO<sub>2</sub> CYCLE




### DISRUPTED PHOTOLYTIC CYCLE

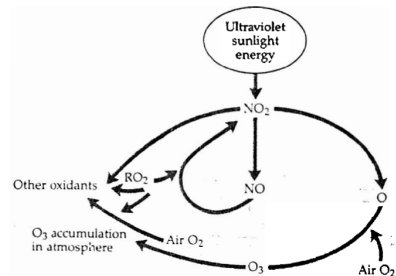


**Figure 23.1**

The production and breakdown of ozone in the lower atmosphere (a) under normal conditions and (b) in the presence of partially oxidized hydrocarbons (RO<sub>2</sub>).



**COLORADO**  
Department of Public Health & Environment

Services & Information Search & commissions Divisions Concerns & emergencies Data News UPhoto

## Air Quality - environmental impacts of cannabis

[Back to Cannabis Industry Environmental Impacts](#)

Growing cannabis emits highly reactive volatile organic compounds (VOCs). Marijuana Infused Product (MIP) facilities also emit VOCs from solvent extraction processes.

Both types of VOCs from the cannabis industry contribute to ozone formation in Denver's ozone nonattainment area. We have recommended best management practices for both grow and MIP facilities to reduce their air quality impacts.

**Environmental impacts**  
Air quality  
Energy resources  
Waste disposal  
Water quality  
Greener Industry Resources

**Cannabis Cultivation Emissions Reduction Fact Sheet**

- Best management practices, Emission reduction tips.

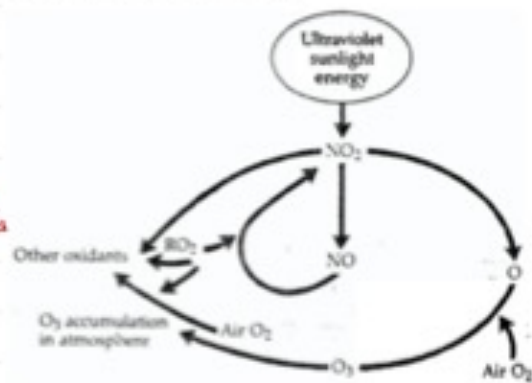
**Solvent Emissions at MIP/Hemp Facilities Compliance Guidance**

- Emission requirements, compliance tips, solvent extraction use.

**In the news**

- The Impact... marijuana grows and extraction labs harm our air... but here's how pollution is being mitigated.

### DISRUPTED PHOTOLYTIC CYCLE



# Atmospheric Composition Affects Atmospheric Chemistry

Increasing tropospheric ozone

Due to  $\text{NO}_x$  ( $\text{NO}$  &  $\text{NO}_2$ ) emissions  
And hydrocarbon emissions

Increasing acid deposition

Due to  $\text{H}_2\text{SO}_4$  &  $\text{HNO}_3$   
Formed from  $\text{SO}_x$  &  $\text{NO}_x$  emissions

# Oxidized N & S gases result from combustion

$\text{NO}_x$  - From fossil fuels,  
biomass, & high temp.  
combustion

$\text{SO}_x$  - From burning of fossil  
fuels

**U.S. Environmental Protection Agency estimates of average passenger car emissions in  
the United States for April 2000<sup>[5]</sup>**

Component	Emission Rate	Annual pollution emitted
Hydrocarbons	2.80 grams/mile (1.75 g/km)	77.1 pounds (35.0 kg)
Carbon monoxide	20.9 grams/mile (13.06 g/km)	575 pounds (261 kg)
$\text{NO}_x$	1.39 grams/mile (0.87 g/km)	38.2 pounds (17.3 kg)
Carbon dioxide - greenhouse gas	415 grams/mile (258 g/km)	11,450 pounds (5,190 kg)

# Tropospheric Ozone has increased in time & space

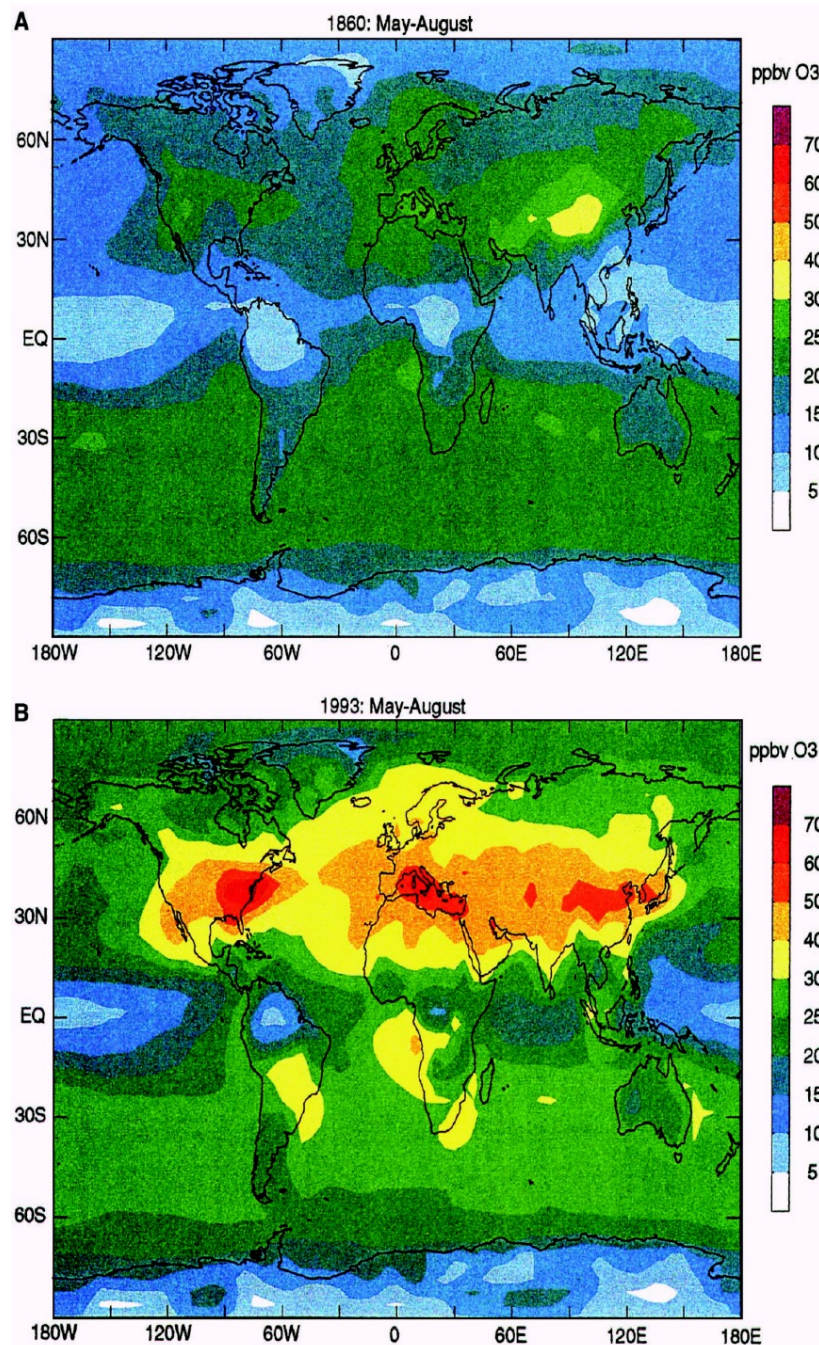
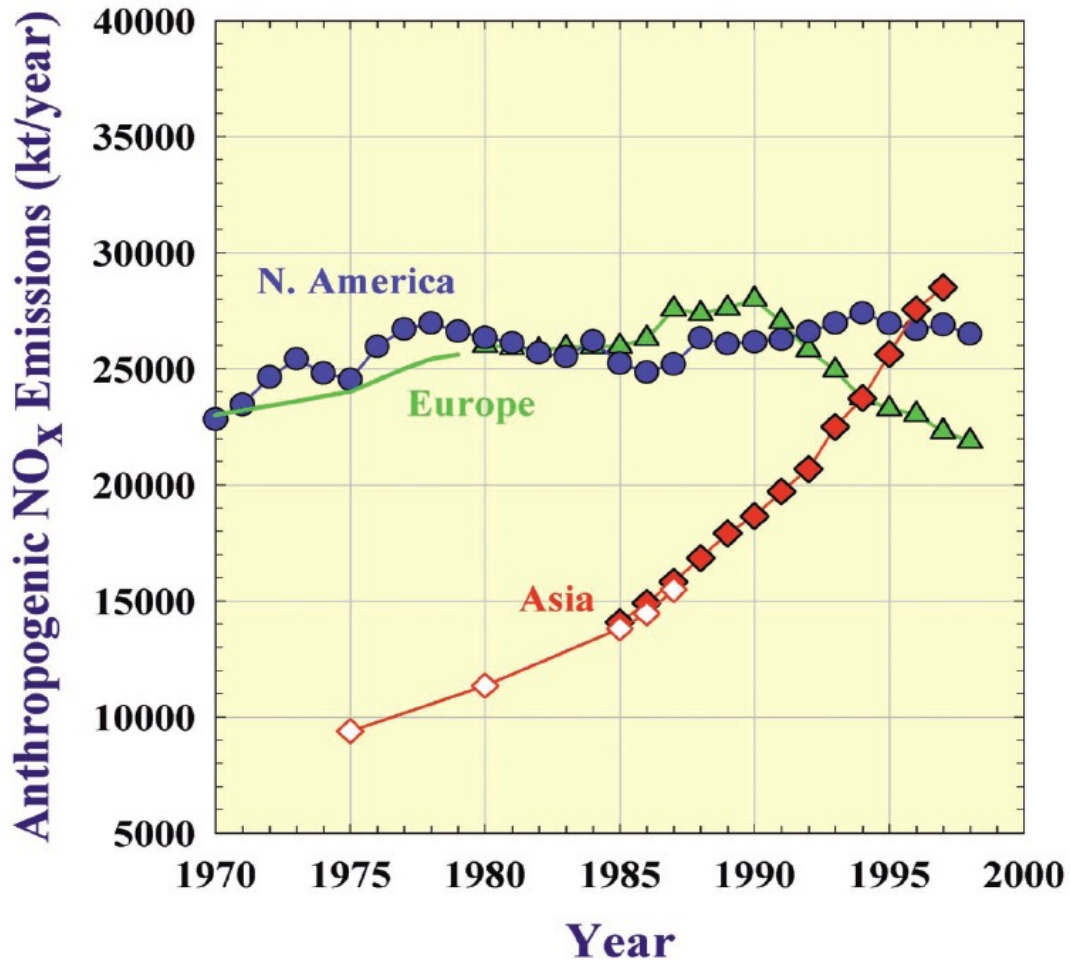


Fig. 1. Model-calculated surface O<sub>3</sub> during the growing season in the Northern Hemisphere (May through August) in (A) 1860 and (B) 1993 (13).

Akimoto 2003

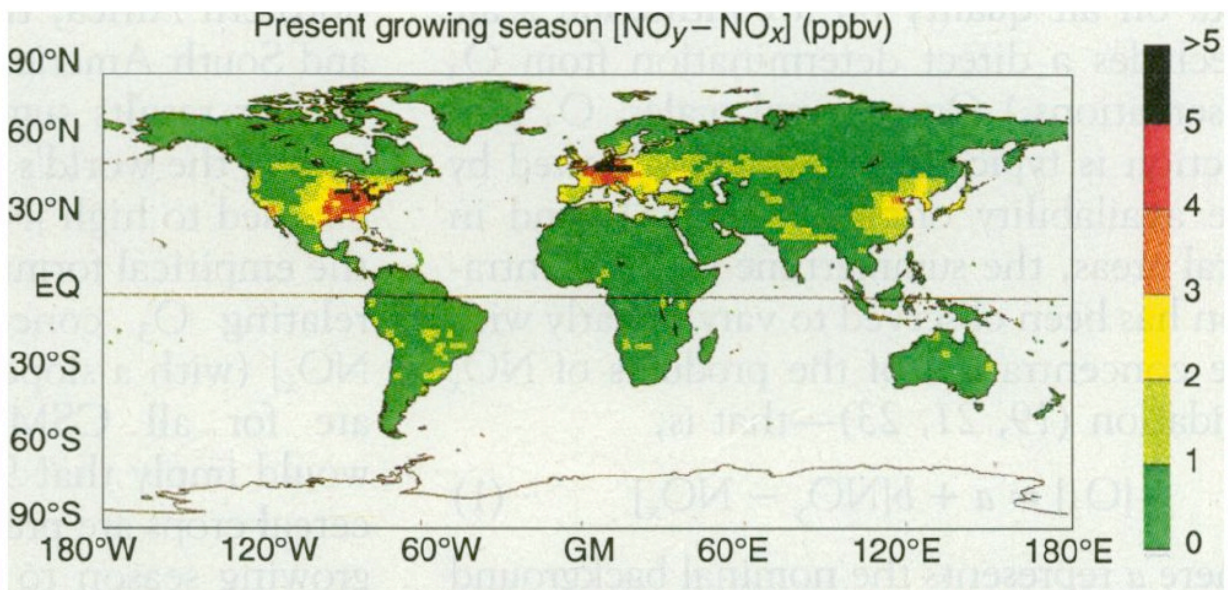
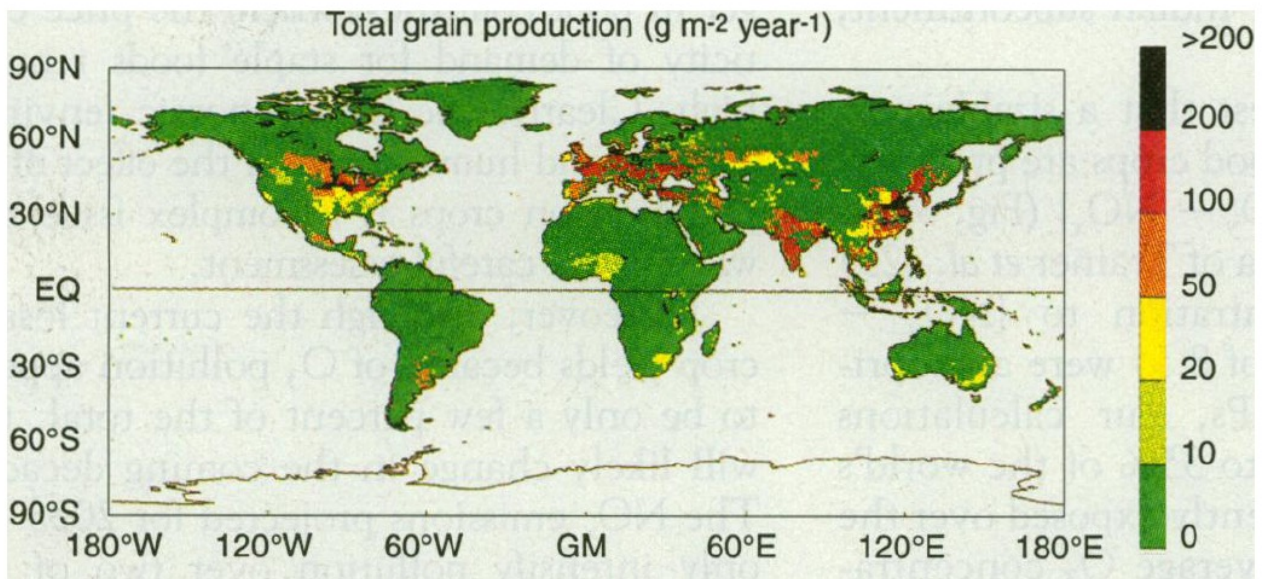


# Tropospheric ozone is likely to continue to increase



Akimoto 2003

**~ 10-35% of the world's grain production  
may occur regions where ozone pollution may  
reduce crop yields**

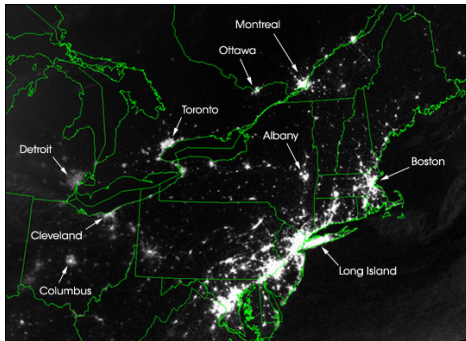


# Atmospheric Chemistry Can Respond to Changes in Pollutant Emissions

GEOPHYSICAL RESEARCH LETTERS, VOL. 31, L13106, doi:10.1029/2004GL019771, 2004

## The 2003 North American electrical blackout: An accidental experiment in atmospheric chemistry

Lackson T. Marufu,<sup>1</sup> Brett F. Taubman,<sup>2</sup> Bryan Bloomer,<sup>1</sup> Charles A. Piety,<sup>1</sup>  
Bruce G. Doddridge,<sup>1</sup> Jeffrey W. Stehr,<sup>1</sup> and Russel R. Dickerson<sup>1,3</sup>



### 24 hours into the blackout

SO<sub>2</sub> down 90%

O<sub>3</sub> down 50%

Visual range up > 40 km

*Over much of the eastern US*

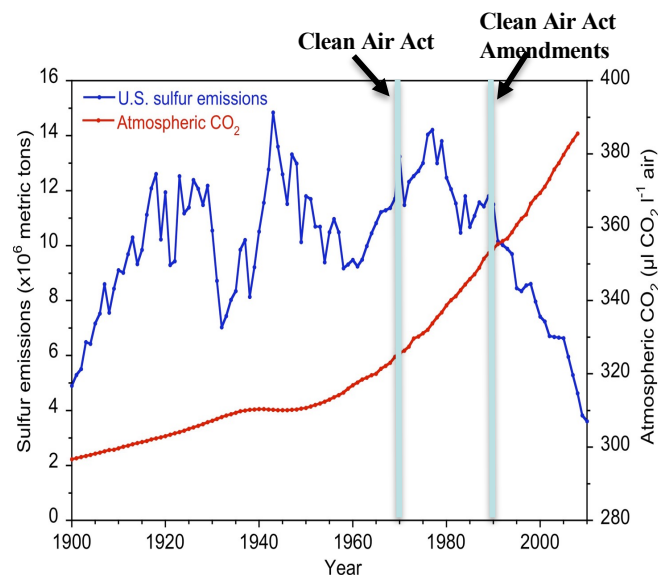
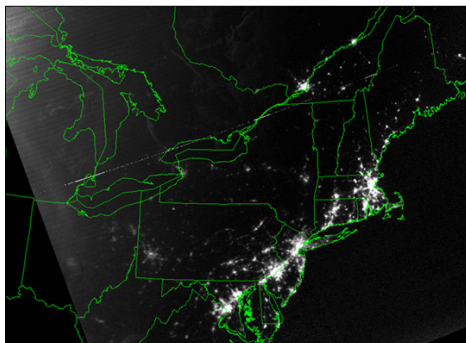
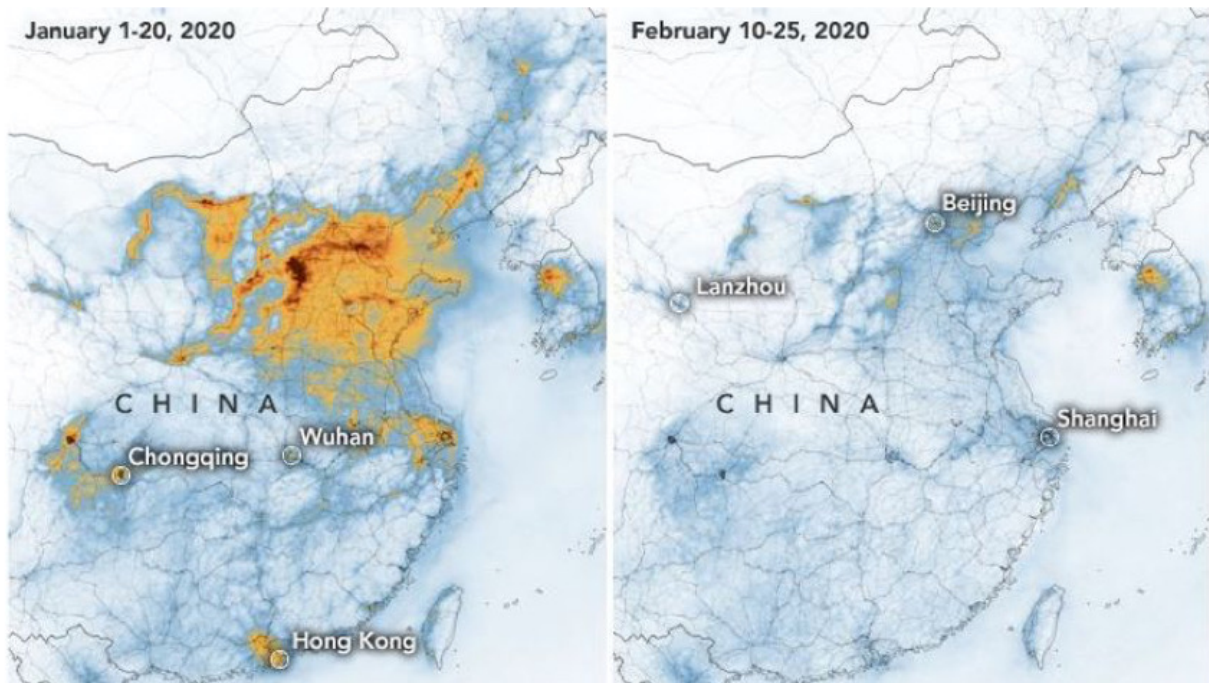


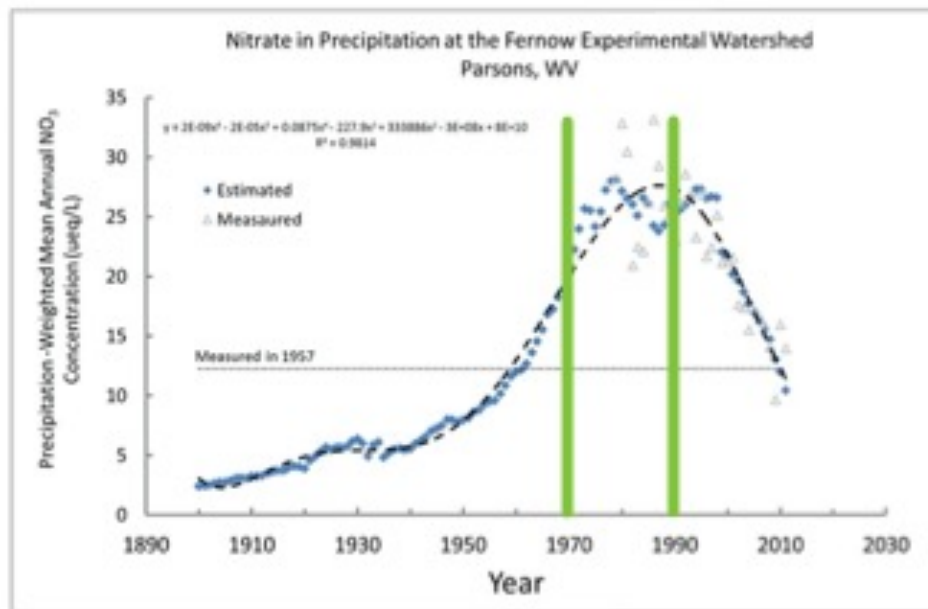
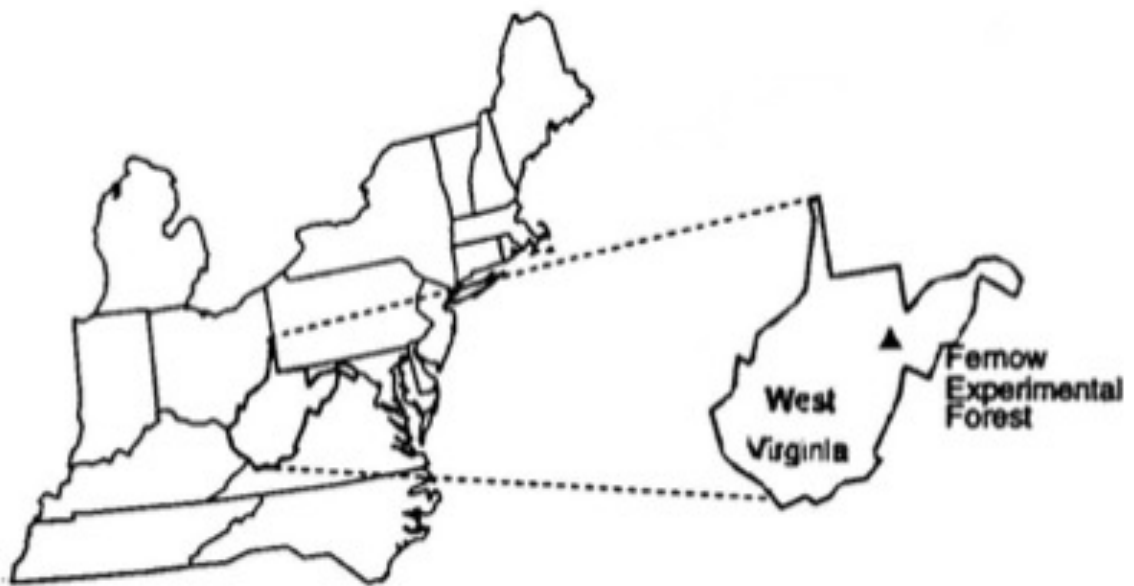
**Figure 1.** Historic sulfur emissions in the U.S. (LeFohn *et al.* 1999) and atmospheric [CO<sub>2</sub>]. There has been a 60% reduction in S deposition in the Central Appalachian Mountains since 1978. From Thomas *et al.* 2013.

## NASA images show coronavirus shutdown has cleared China pollution

The US space agency says travel restrictions and the closure of businesses contributed to the drop in nitrogen dioxide.

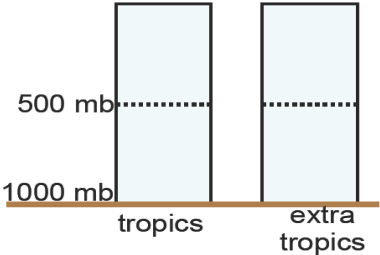


<https://news.sky.com/story/nasa-images-show-coronavirus-shutdown-has-cleared-china-pollution-11946759>

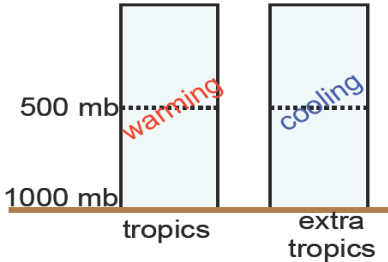


# Types of Atmospheric Circulation

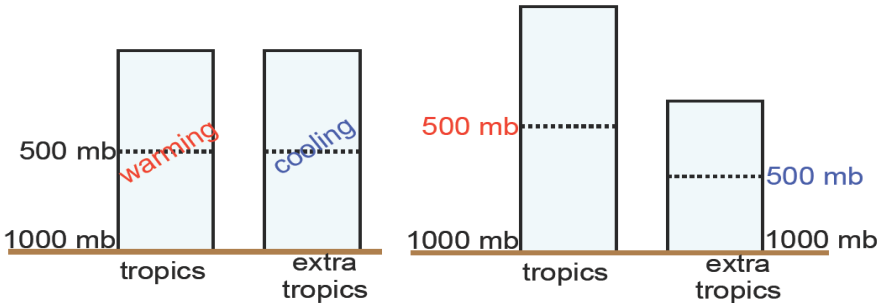
# Consider two columns of air, one warming and the other cooling



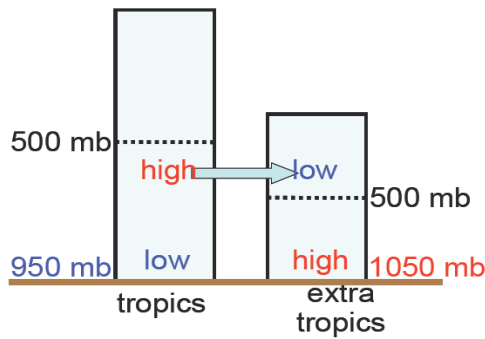
*assume initially they are the same*



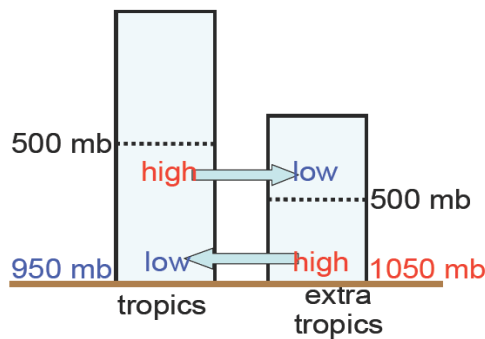
*what will happen to the columns?*



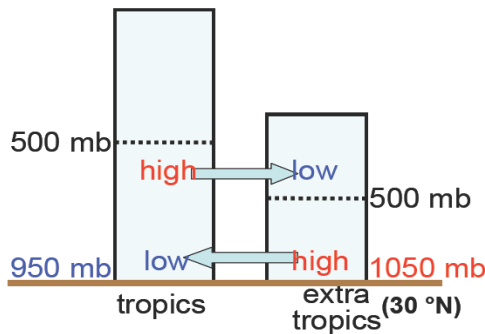
# What happens next?



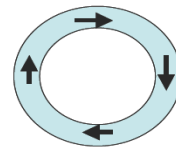
- 1) *air has moved out of tropics*
- 2) *pressure is related to mass of atm. above, so tropical surface pressure decreases*



- 1) *air has moved out of tropics*
- 2) *pressure is related to mass of atm. above, so tropical surface pressure decreases*
- 3) *air moves from high to low pressure at the surface*



*these are the forces that drive the circulation of the Hadley cells*



*northern limb*

Hadley Cell



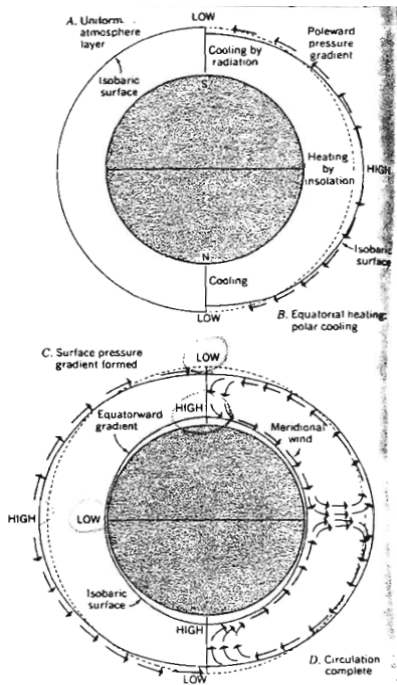


Figure 4.6 Convective wind system on an imagined nonrotating earth. (From A. N. Strahler, 1971, *The Earth Sciences*, 2nd ed., Harper & Row, New York.)

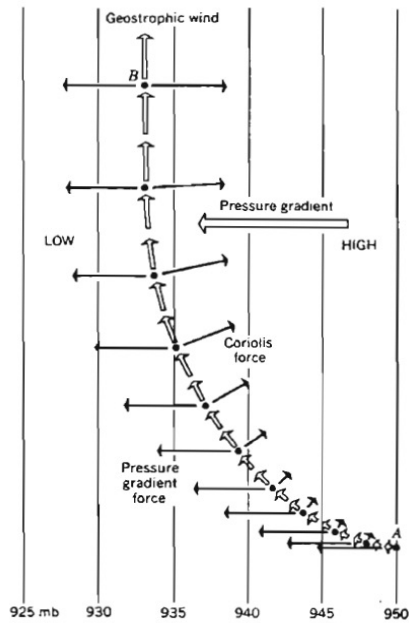


Figure 4.8 Deflection of a parcel of air by the Coriolis force, leading to development of the geostrophic wind. (From A. N. Strahler, 1971, *The Earth Sciences*, 2nd ed., Harper & Row, New York.)

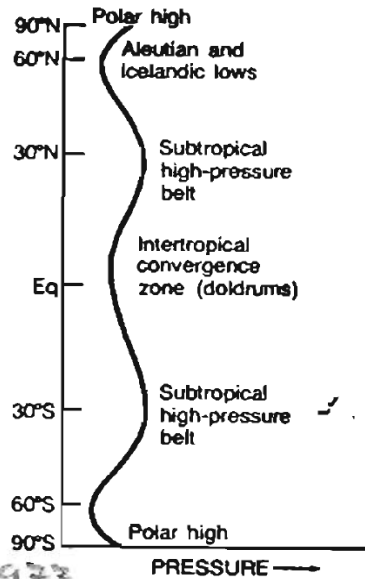


FIGURE 2-22 Variation of average sea-level pressure with latitude. (From Neiburger, Edinger, and Bonner, 1973.)

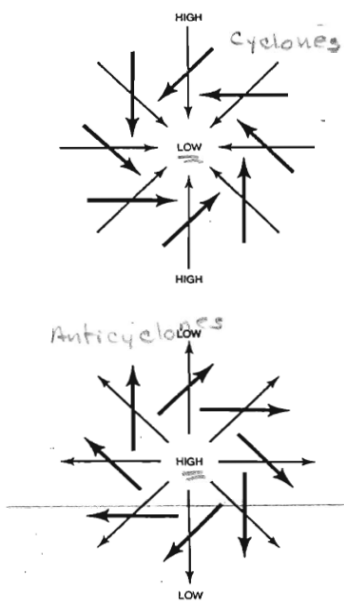


FIGURE 2-19 Coriolis deflection of the wind. Light arrows denote the direction of pressure-gradient force, which would also be wind direction on a nonrotating Earth. Heavy arrows show the Coriolis deflection of the wind directly to the right (Northern Hemisphere).

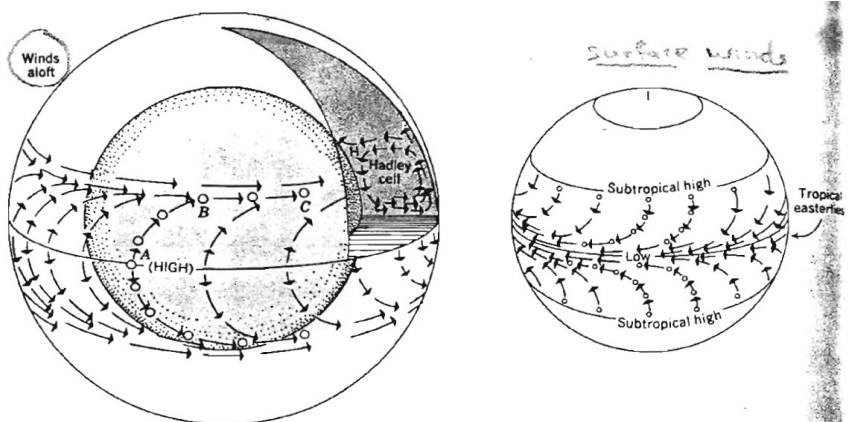
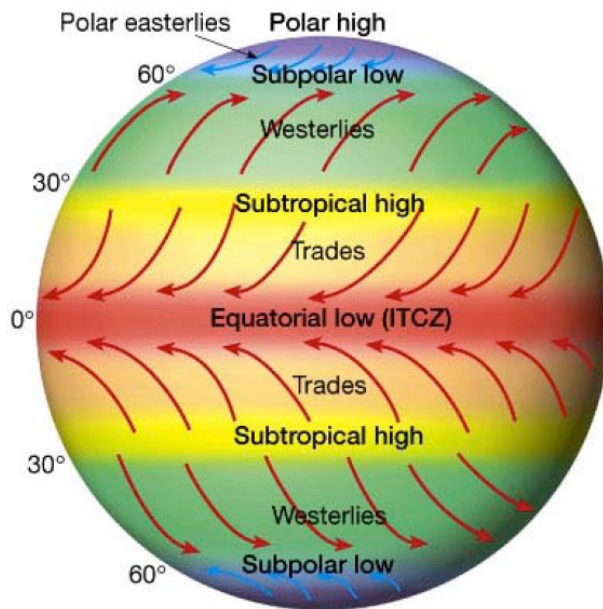
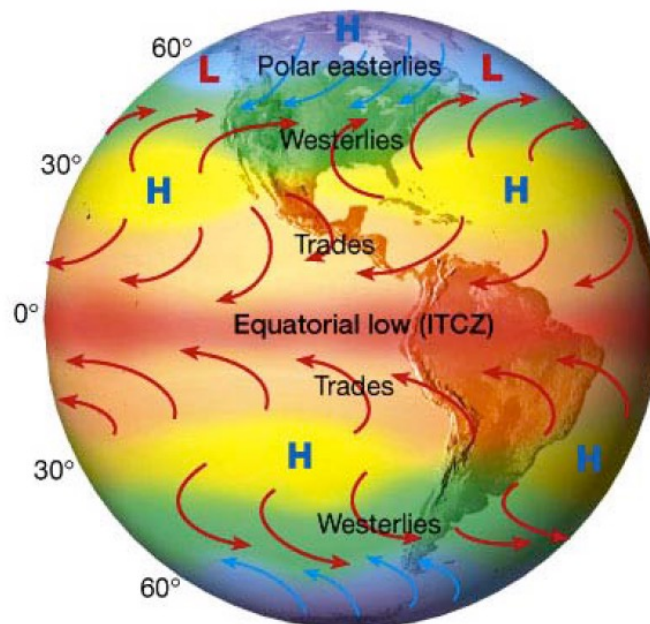


Figure 4.13 Idealized diagram of formation of the Hadley cell circulation and the tropical easterlies. (From A. N. Strahler, 1971, *The Earth Sciences*, 2nd ed., Harper & Row, New York.)

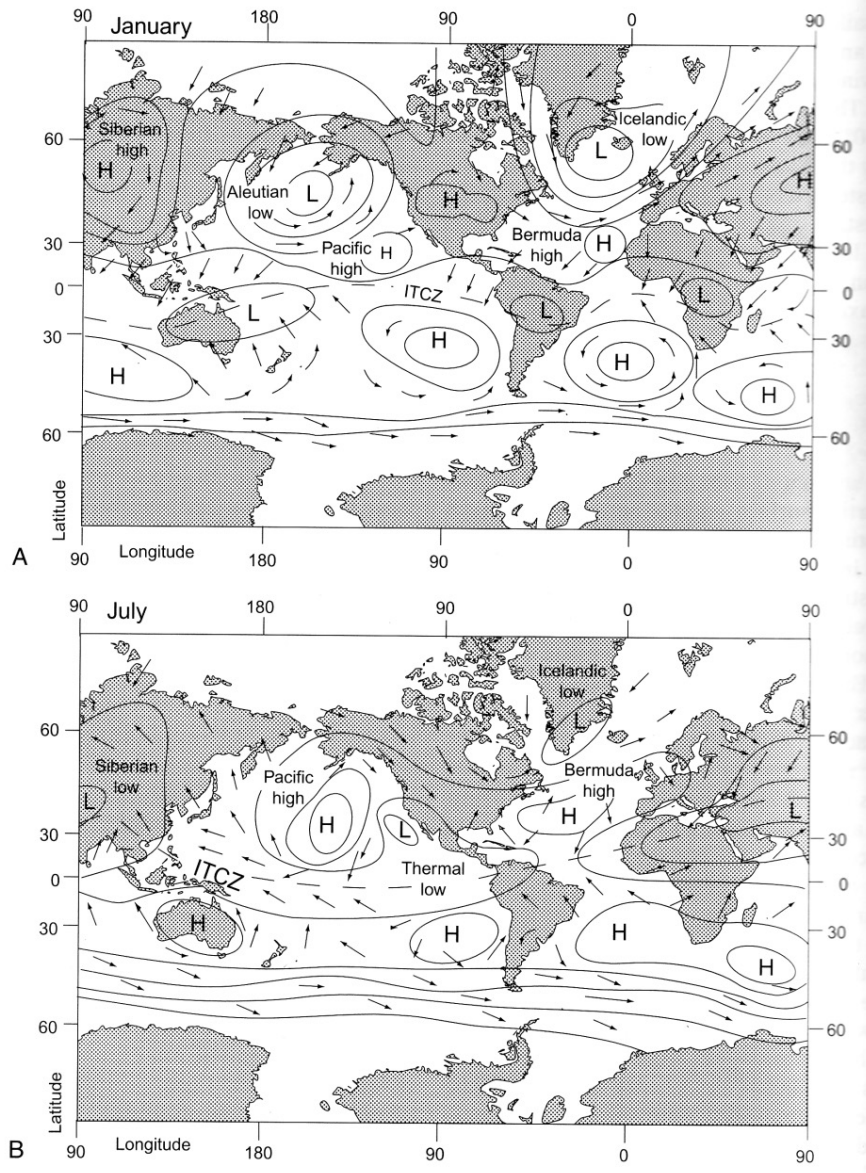
## Pattern of General Circulation of Surface Winds



Surface pressure “belts” become cells in response to differential heating of land and sea and physical barriers to flow.



# Cyclonic Circulation



From Chapin et al. 2002

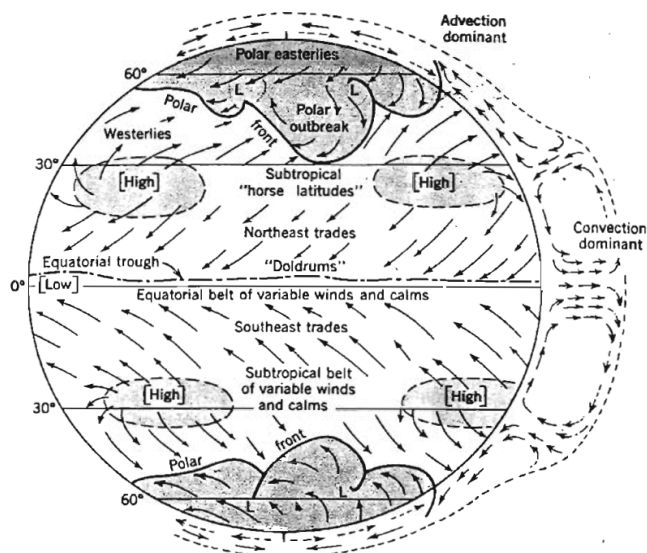
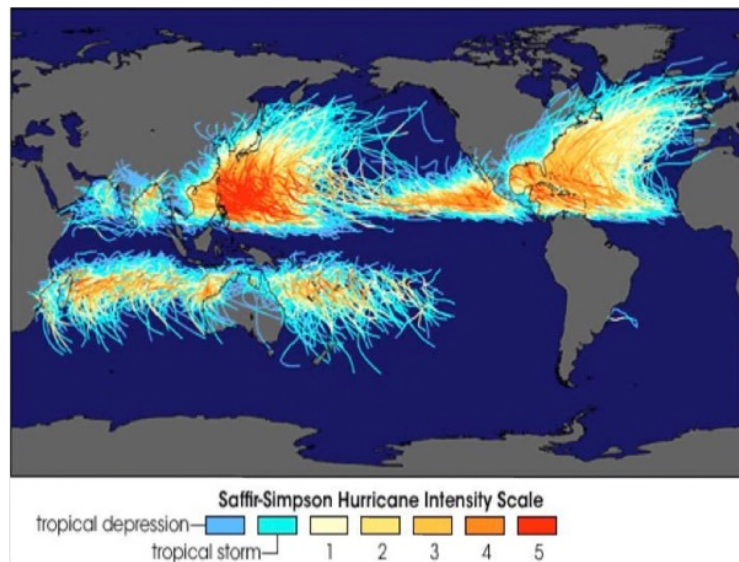


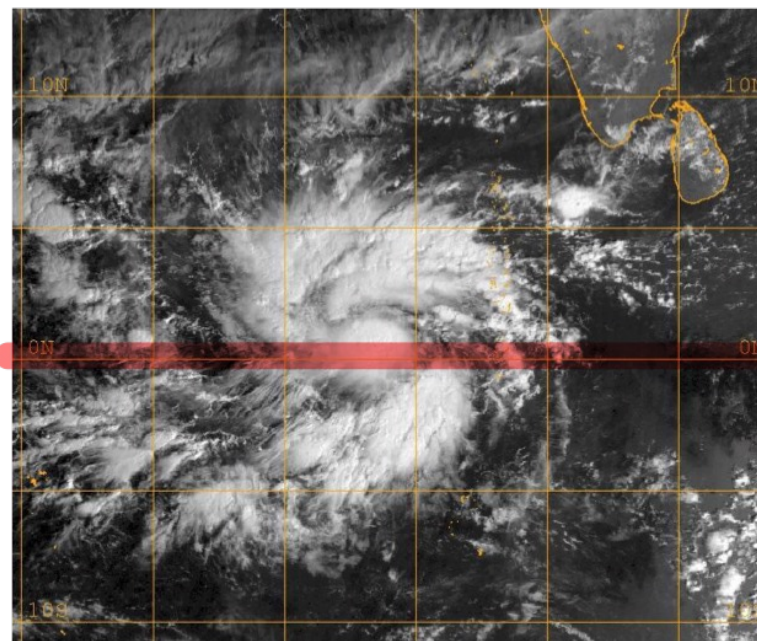
Figure 4.26 Idealized diagram of global surface winds.

S. Brakenbury 1973

Hurricanes (Atlantic basin, E. Pacific), typhoons (W. Pacific), and cyclones (Indian Ocean, Australia) rarely if ever form between 5 deg North and 5 deg South latitudes, respectively



150 years of tropical cyclone tracks through 2006.  
NASA EARTH OBSERVATORY



2004 cyclone Agni